

ON THE EFFICIENCY OF A CYCLOIDAL PLANETARY REDUCER WITH A MODIFIED STRUCTURE

Mircea NEAGOE*, Dorin DIACONESCU*, Lucia PASCALE**, Radu SĂULESCU*

* “Transilvania” University of Braşov, Romania,

** “Valahia” University of Târgovişte, Romania

Abstract. The paper deals with a new variant of a cycloidal reducer with modified structure, proposed by the authors, able to accomplish high transmission ratio and high efficiency. Based on a reducer physical prototype and using a modern high-tech stand, experimental researches on the efficiency in several relevant functioning cases were performed. The obtained experimental results comply with the theoretical model, and some performance features of the reducer prototype are thus derived.

Keywords: cycloidal planetary reducer, efficiency, internal efficiency, transmission ratio, experimental testing

1. Introduction

A new variant of planetary cycloidal reducers, equipped with one sun gear, proposed by the authors, is illustrated in figure 1; it contains a cycloidal gear pair with rollers, consisting of a base fixed sun gear with internal cycloidal teeth 3 and of more rollers 2. The element H (which contains an eccentric bearing) designates the reducer's *input*, while the element 1 (on which the rollers 2 are eccentrically articulated) designates the *output*.

In the premise that the reducer uses $z_2 = 16$ rollers (as teeth), then $z_3 = z_2 + 1 = 17$ teeth and, implicitly, the reducer accomplishes the *kinematical transmission ratio* [3, 5]:

$$i_{H1}^3 = \frac{\omega_{H3}}{\omega_{13}} = \frac{\omega_{3H}}{\omega_{3H} - \omega_{1H}} = \frac{1}{1 - \frac{\omega_{1H}}{\omega_{3H}}} = \frac{1}{1 - i_0} = -16 \quad (1)$$

in which

$$i_0 = i_{13}^H = i_{12}^H \cdot i_{23}^H = +1 \cdot \left(+ \frac{z_3}{z_2} \right) = +1.0625 \quad (2)$$

is the *internal ratio* of the planetary unit.

In the assumption of friction considering, the reducer efficiency η_{H1} can be theoretically established through the following relation:

$$\eta_{H1} = \frac{-T_1 \cdot \omega_{13}}{T_H \cdot \omega_{H3}} = \frac{-T_1}{T_H} = \frac{i_{H1}^3}{i_{H1}^3} = \frac{1 - i_0}{1 - i_0 \cdot \eta_0^w} \quad (3)$$

where T_H and T_1 are the input and respectively output torque, η_0 is the reducer *internal efficiency* ($\eta_0 = \eta_{13}^H = \eta_{12}^H \cdot \eta_{23}^H$), and w – the efficiency

coefficient ($w = \pm 1$) that models the power circulation in the fixed axis unit associated to the planetary unit [2, 3]:

$$w = \text{sgn}(\omega_{1H} \cdot T_1) = \text{sgn} \left(\frac{\omega_{1H} \cdot T_1}{-\omega_{13} \cdot T_1} \right) = \text{sgn} \left(\frac{\omega_{1H}}{\omega_{3H} - \omega_{1H}} \right) = \text{sgn} \left(\frac{i_0}{1 - i_0} \right) = \text{sgn} \left(\frac{17/16}{1 - (17/16)} \right) = -1 \quad (4)$$

The paper deals with the reducer *efficiency* η_{H1} (see rel. 3) experimentally established based on the measurement of the input and output torques (T_H and T_1) and of their corresponding rotational speeds (ω_{H3} and ω_{13}); by means of the obtained *efficiency* η_{H1} , the *reducer internal efficiency* η_0 is thus determined:

$$\eta_{H1} = \frac{1 - i_0}{1 - i_0 \cdot \eta_0^{-1}} \Rightarrow \eta_0 = \frac{i_0 \cdot \eta_{H1}}{i_0 - (1 - \eta_{H1})} \quad (5)$$

Complying with previous stated objectives, in the paper will be further briefly presented the stand used in experimental testing (section 2), the experimental research planning and the obtained results (section 3), and final conclusions (section 4).

2. The Testing Stand

Experimental identification of the efficiency of the new proposed cycloidal reducer is based on the numerical data (torques and rotational speeds values) supplied by a specialized mechatronic stand developed at Product Design and Robotics Department of Transilvania University Brasov, schematically presented in figure 2 [7].

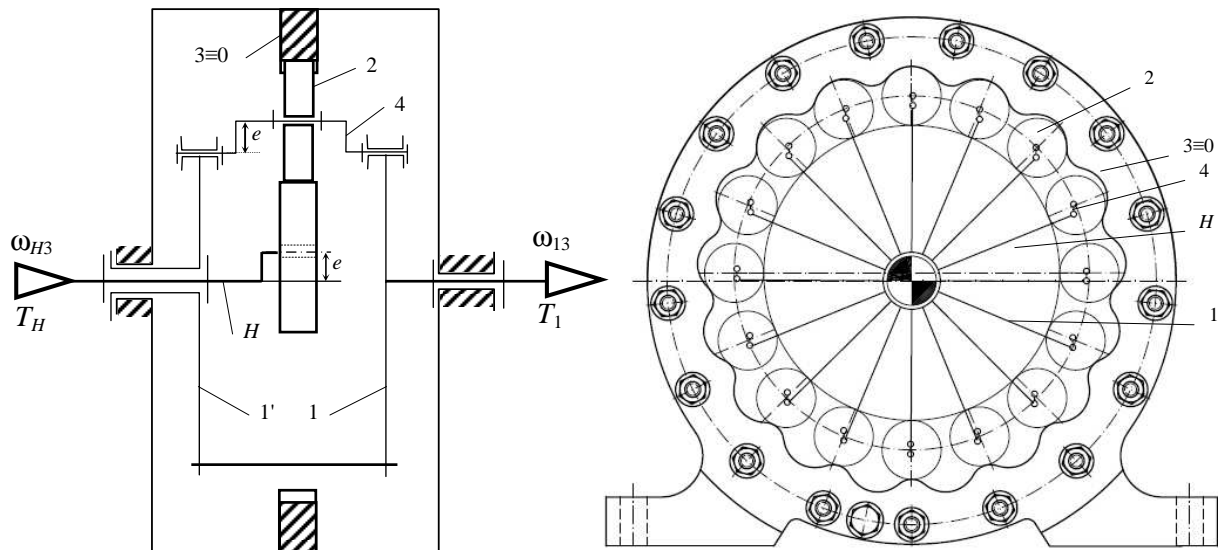


Figure 1. The cycloidal reducer equipped with a sun gear (3) and eccentric rollers (2)

One of the main stand component is designed by two synchronous brushless servomotors Siemens 1FT6-105, controlled with the aid of two Siemens 6SE7023 PWM invertors. The servomotors can operate as motor or brake (figure 3,a) and are characterized by the following features: nominal/maximum torque: 31/41 Nm; maximum speed: 3000 rot/min; nominal power: 9.4 kW.

The sensorial system of the mechatronic stand (figure 2 and figure 3,b) is composed by two T20WN/200Nm HBM torque-speed transducers which can be used to measure both static and

dynamic torques and a maximum rotational speed of 10000 rot/min, two PCB 356A15 three-axial shear accelerometers able to measure accelerations up to $\pm 490 \text{ m/s}^2$. An external acquisition device HBM Spider 8 is used to gather all the signals from the external sensors. Spider 8 is a modular 12 bit resolution acquisition system with 4 channels and a 4.8 kHz carrier frequency.

The whole testing system is controlled by the human operator through a PC which is linked with the servomotor's controllers by RS-232/RS-485 card interface, used to send the reference digital

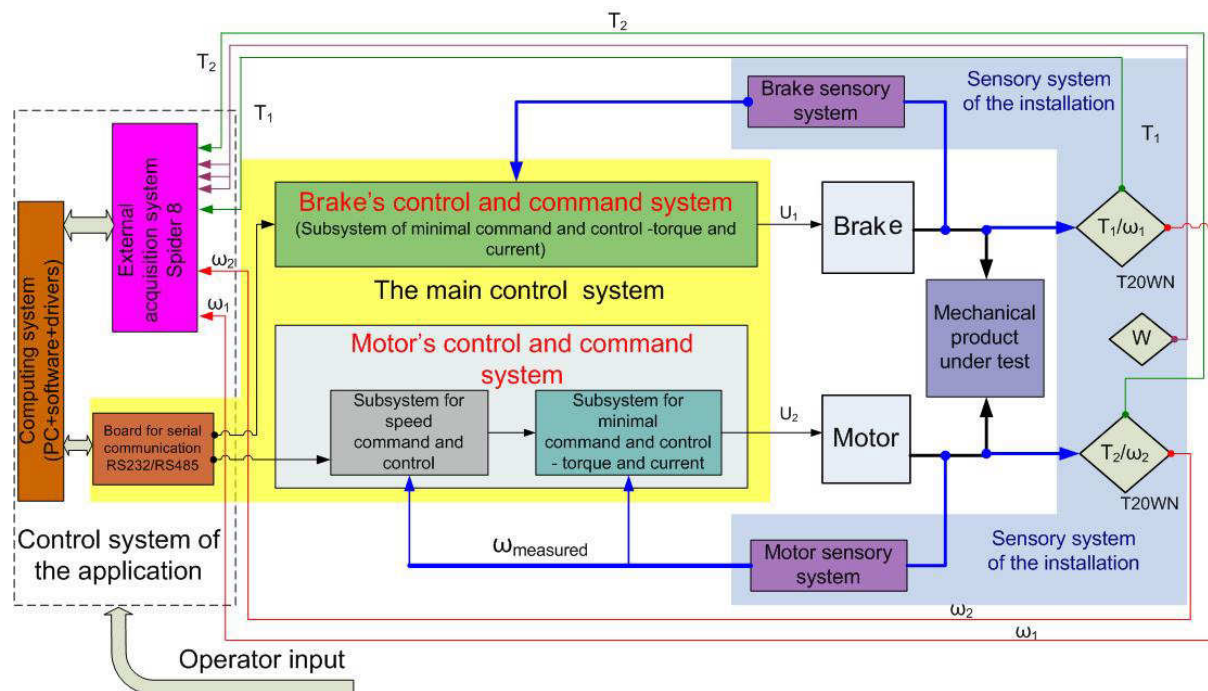


Figure 2. Scheme of the mechatronic stand used in experimental testing of reducer efficiency [7].

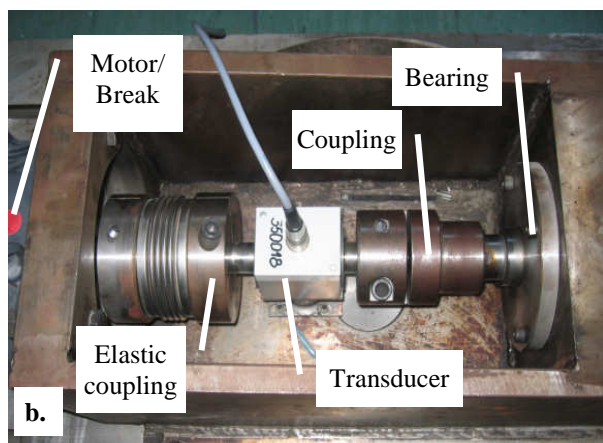
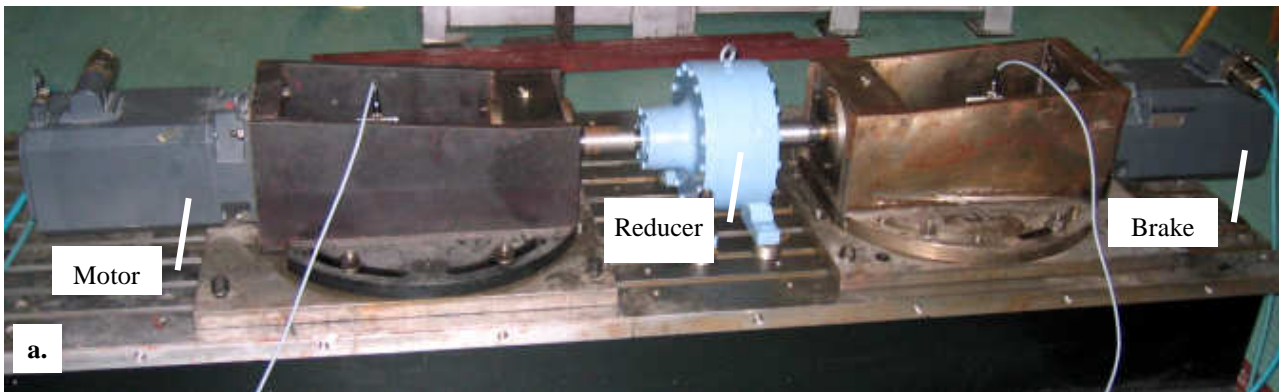


Figure 3. The stand-reducer system:
a) general view, b) stand sub-components

- the motor rotational speed was successively commanded at the values: 320; 960 and 1600 [rot/min],
- for each commanded motor speed, in case a), the brake was loaded successively at the following torque values: 0; 32 and 40 [Nm],
- the experimental data (torque and speed) delivered by both stand transducers were recorded and the average experimental values of speed (n_M – motor average speed, and n_B – brake average speed) and of torque (namely T_M and respectively T_B) were established, for each functioning case.

C. In the cases of load running regime ($T_b > 0$) from the functioning situation a):

- there were established the input torque ($T_M = T_H$) and the output torque ($T_B = T_1$) of the reducer,
- the *efficiency* (η_{H1}) was computed in the known *classical assumption*: there are considered only the mechanical energy losses due to the friction in cycloidal gear and in the revolute joints of the reducer radial coupling (see figure 1); in this respect, the energy losses from shaft bearing, the energy needed for lubricant barbotage etc. are neglected.
- finally, the interior efficiency (η_0) was established for each distinct operating case, based on the values previously computed of the *efficiency* η_{H1} (see rel. 5).

For a correct interpretation of the numerical results obtained from the performed testing and to comply with the classical assumption, it must make evident the mechanical energy losses in the mechatronic stand subcomponents (see figures 2 and 3): **motor** – elastic clutch – transducer – rigid coupling – bearing – **reducer** – bearing – rigid coupling – transducer – elastic clutch – **brake**.

signal and to receive status information about servomotors (figure 2). Also the PC is linked to the acquisition external device via the parallel or the COM port depending on the amount of data that needs to be transferred. The command system implemented on the PC allows a discrete (point-to-point) or continuous changing of the time variable parameters. In the mechatronic stand, a servomotor is functioning as motor, with speed control, while the other is operating as brake (torque control).

3. Experimental Planning

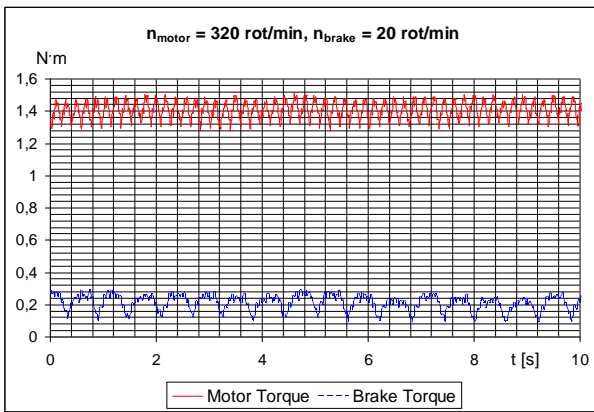
The testing program of the reducer prototype efficiency, using the stand previously described (see figure 3), is based on the following algorithm [6]:

A. There were recorded (experimental data delivered by torque-speed transducers):

a) instantaneous torque/speed values of the system motor-reducer-brake, in both cases of idle-running regime ($T_b = 0$) and load running regime ($T_b > 0$);

b) instantaneous torque/speed values of each servomotor subsystem (operating as motor), decoupled from the reducer and no load at the output shaft.

B. For each of two previous mentioned working situations a) and b):

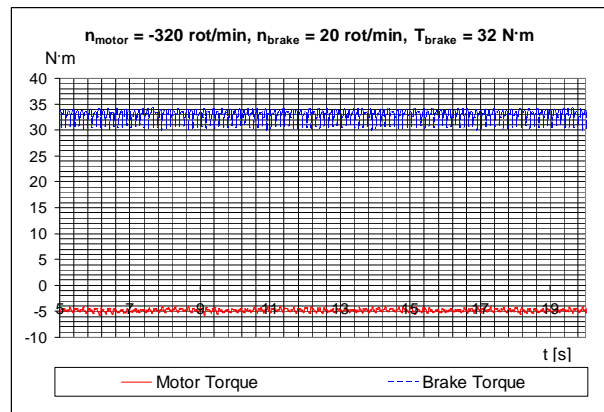


a.

Average speed [rot/min]		Average torque [N·m]	
Motor n_M	Brake n_B	Motor T_{M1}	Brake T_{B1}
315,29170	-24,87196	1,38455	0,20100
960,53066	-59,49240	1,60468	0,35247
1601,9406	-98,49149	1,65059	0,48314

b.

Figure 4. The torques and speeds recorded by the stand transducers in the case of servomotors decoupled from the reducer: example of data records (a) and the average values of speed and torque obtained by processing the experimental recorded data (b)

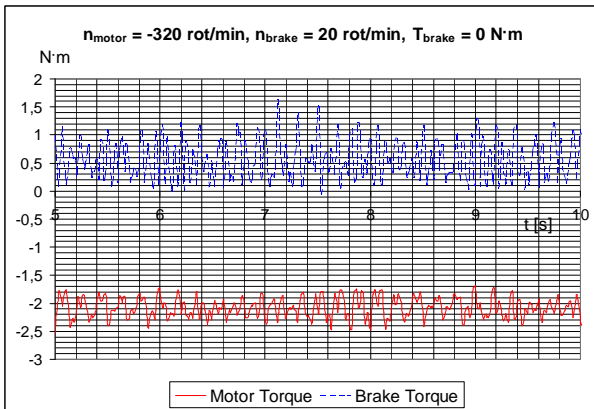


a.

Average speed [rot/min]		Average torque [N·m]	
Motor n_M	Brake n_B	Motor T_{M4}	Brake T_{B4}
-320,02721	20,06838	-4,79151	32,62090
-960,12467	60,15845	-5,82169	32,74974
-1600,1638	100,03003	-6,78839	32,57805

b.

Figure 6. The torques and speeds recorded by the stand transducers in the case of servomotors coupled to the reducer and the brake load is $T_{Brake} = 32$ Nm: example of data records (a) and the average results obtained by processing the experimental recorded data (b)

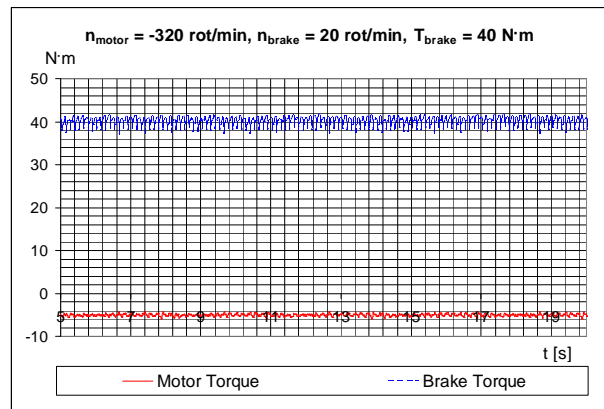


a.

Average speed [rot/min]		Average torque [N·m]	
Motor n_M	Brake n_B	Motor T_{M2}	Brake T_{B2}
-319,99200	20,02330	-2,07230	0,49384
-959,94647	60,01714	-3,02167	0,25328
-1599,8953	99,98878	-4,38306	0,48445

b.

Figure 5. The torques and speeds recorded by the stand transducers in the case of servomotors coupled to the reducer and no brake load (idling): example of data records (a) and the average results obtained by processing the experimental recorded data (b)



a.

Average speed [rot/min]		Average torque [N·m]	
Motor n_M	Brake n_B	Motor T_{M4}	Brake T_{B4}
-319,99545	20,01840	-5,08105	39,93556
-960,05081	60,07087	-6,10078	40,28985
-1600,0849	99,94924	-7,45981	40,31668

b.

Figure 7. The torques and speeds recorded by the stand transducers in the case of servomotors coupled to the reducer and the brake load is $T_{Brake} = 40$ Nm: example of data records (a) and the average results obtained by processing the experimental recorded data (b)

The records performed on each servomotor subsystem, decoupled from the reducer (stage I), are shown in figure 4,a for $n_{motor} = 320$ rot/min and $n_{brake} = 20$ rot/min. These experimental data, obtained while each servomotor is operating as motor, allow us to identify the energy losses due to the bearing friction (see figure 3,b), where T_{M1} and T_{B1} (figure 4,b) represent the *average torques* recorded by the motor transducer and respectively brake transducer.

In the second stage were also recorded the torque and speed experimental values delivered by the stand transducers, for the case of: *reducer coupled to the servomotor subsystems, no brake load, and the motor speed commanded successively to: a) 320, b) 960 and c) 1600* [rot/min]. The average values of the obtained torques and speeds are systematized in figure 5,b, while the time variation of instantaneous torques is exemplified in the figure 5,a for the case of $n_{motor} = 320$ rot/min.

Similarly, in the third stage were recorded the instantaneous torques and speeds for the case of *reducer coupled to the servomotor subsystems, the motor speed commanded successively to: a) 320, b) 960 and c) 1600* [rot/min], and the brake successively loaded at 32 [N·m] (figure 6,b) and 40 [N·m] (figure 7,b); the records of instantaneous torques are exemplified for $n_{motor} = 320$ rot/min and $T_{brake} = 32$ [N·m] (figure 6,a) and respectively $T_{brake} = 40$ [N·m] (figure 7,a).

The oscillations of the motor torques and especially of the brake torques (figures 4, 5, 6 and 7), with increased amplitude and frequency at higher speeds, are generated mainly by a certain disequilibrium of the input shaft H , combined with certain manufacture inaccuracy of the cycloidal tothing.

Based on results shown in figures 4 and 5, for the idling stage, the average residual output torques ($T_{B3} = T_{B2} + T_{B1}$) and average residual input torques ($T_{M3} = T_{M2} - T_{B3}/i_{H1}/\eta_{H1}$) of the reducer were established and systematized in table 1.

Table 1. The average residual input torques T_{M3} and average residual output torques T_{B3} of the reducer

Average speed [rot/min]		Average residual torque [N·m]	
Motor n_M	Brake n_B	Motor $T_{M3}=T_{M2}-T_{B3}/(i_{H1}/\eta_{H1})$	Brake $T_{B3}=T_{B2}+T_{B1}$
-319.99200	20.02330	-2.017264	0.694844
-959.94647	60.01714	-2.973733	0.605766
-1599.8953	99.98878	-4.306514	0.967600

The reducer input residual torque represents, in conformity with its formula ($T_{M3} = T_{M2} - T_{B3}/i_{H1}/\eta_{H1}$), the motor torque needed

to operate the reducer in the idling stage; because only the friction losses from cycloidal gear and from transversal coupling joints are commonly considered in the efficiency practice, the loss of energy corresponding to the residual input torque should be neglected. Hence, with the aim to comply to the current theoretical premises, the residual input torque will be eliminated from the efficiency calculus and thus the direct comparison between efficiency of the tested cycloidal prototype and of other existing gears becomes possible.

Based on previous assumptions, the average values of the reducer input/output speeds (namely n_M/n_B) and torques (namely T_M/T_B), together with the reducer efficiency for the tested load-running regime, are systematized in table 2. The efficiency values η_{H1} , established in the condition to comply with the theoretical premises, were computed with the expression $\eta_{H1} = (T_B/T_M)/(n_M/n_B) = (T_B/T_M)/i_{H1}$. Moreover, the internal efficiency η_0 (see rel. 5) is derived for each corresponding efficiency value η_{H1} , yielding for all the 6 tested regimes to an average value $\eta_{0med} = 98.45\%$. Comparing the internal efficiency of the tested prototype with the efficiency of the evolventic gears with milled tothing ($\eta = 96\% - 97\%$ [1, 4]), it can be emphasized that the new proposed reducer has, beside other advantages (simple technology, reduce costs), a superior energetic performance ($\eta_{0med} = 98.45\%$).

4. Conclusions

According to the previous remarks, the following final conclusions can be drawn:

1. A modern mechatronic stand of motor-reducer-brake type with open power flow was used to test the new proposed reducer prototype. This stand, that includes modern control and monitoring equipments, is located at Product Design and Robotics Department from "Transilvania" University of Brasov.

2. Several testing running regimes were performed and the corresponding instantaneous experimental torques and speeds were recorded. We considered the following testing configurations: a) idle-running regime, servomotors decoupled from the reducer; b) running the system motor-reducer-brake with various motor speeds and no brake load; c) running the system motor-reducer-brake with various motor speeds and various brake loads. The average torques and average speeds were established for all the testing regimes.

Table 2. The reducer experimental efficiency

Average speed [rot/min]		Average torque [N·m]		Efficiency [%]	
Motor n_M	Brake n_B	Reducer input torque $T_M = T_{M4} - T_{M3}$	Reducer output torque $T_B = T_{F4} + T_{F1}$	η_{H1}	η_0
-320.0272147	20.06838119	-2.7742519	32.821904	74.190%	97.995%
-319.9954574	20.01840823	-3.0637931	40.136568	81.953%	98.721%
-960.1246776	60.15845723	-2.8479589	33.102226	72.827%	97.852%
-960.0508001	60.07087449	-3.1270503	40.642328	81.323%	98.667%
-1600.163832	100.03003267	-2.4818796	33.061200	83.273%	98.832%
-1600.084905	99.94924773	-3.1533046	40.799834	80.822%	98.623%
Average values:				79.064%	98.64%

3. The efficiency values were computed from the experimental data, in the compatibility conditions of the theoretical premises currently used in practice. The oscillations of instantaneous torques in the stationary state are generated mainly by the disequilibrium of the input shaft H , combined with certain manufacture inaccuracy of the cycloidal toothing; these oscillations are amplified while the motor speed is increased.

4. The obtained experimental efficiency (in the conditions of the foremost prototype, where the cycloidal toothing was manufactured using a classical milling machine) attests the energetic superiority of the proposed reducer solution versus the evolventic solutions (in similar technological and functional conditions).

References

1. Chişiu, A. et al.: *Machine elements*. “Didactică și Pedagogică” Publishing House, Bucharest, Romania, 1976, (in Romanian)
2. Diaconescu, D.: *Conceptual Design*. “Transilvania” University Press, Brasov, Romania, 2005, ISBN 973-635-544-6 (in Romanian).
3. Miloiu, G., Dudiță, FL., Diaconescu, D.V.: *Modern Mechanical Transmissions*. “Tehnică” Publishing House, Bucharest, Romania, 1980 (in Romanian)
4. Nasui, V., Pay, G.: *Basis of mechanical efficiency optimization*. North University Press of Baia Mare, Romania, 2000, ISBN 973-99543-4-0 (in Romanian)
5. Neagoe, M., Diaconescu, D.: *Mechanisms. Structure analysis and gear mechanisms*. “Transilvania” University Press, ISBN 973-635-3125, Braşov, Romania, 2004 (in Romanian)
6. Pascale, L.: *Comparative analysis of modern planetary gears and a new reducer synthesis*. PhD Thesis, “Transilvania” University of Braşov, Romania, 2007 (in Romanian)
6. Şişcă, S., Mogan, G.: *Modular test bench used as a versatile tool in the mechanical product design cycle*. The 6th International Conference "Research and Development in Mechanical Industry", RaDMI 2006, September 2006, ISBN 86-83803-21-X (HTMS)